CARBON NANOTUBES BAND ASSIGNATION, TOPOLOGY, BLOCH STATES AND SELECTION RULES

T. Vuković† and I. Milošević and M. Damnjanović

Faculty of Physics, University of Belgrade, POB 368, Beograd 11001, Yugoslavia

(Dated: May 21, 2001)

Various properties of the energy band structures (electronic, phonon, etc.), including systematic band degeneracy, sticking and extremes, following from the full line group symmetry of the single-wall carbon nanotubes are established. The complete set of quantum numbers consists of quasi momenta (angular and linear or helical) and parities with respect to the z-reversal symmetries and, for achiral tubes, the vertical plane. The assignation of the electronic bands is performed, and the generalized Bloch symmetry adapted eigen functions are derived. The most important physical tensors are characterized by the same set of quantum numbers. All this enables application of the presented exhaustive selection rules. The results are discussed by some examples, e.g. allowed interband transitions, conductivity, Raman tensor, etc.

PACS numbers: 71.20.Tx, 63.22.+m, 61.48.+c

I. INTRODUCTION

It is well known that the single-wall carbon nanotubes[1] (SWCT) besides the translational periodicity along the tube axis (z-axis, by convention) possess a screw axis and pure rotational symmetries. Consequently, in calculations of the electronic energy band structure the conserved quantum numbers of linear[2] k, or helical[3] $\tilde{k}$, quasi momenta together with z-projection of the orbital angular momentum (related to rotational symmetries) are used. On the contrary, the parity quantum numbers following from the full line group symmetry[4] including horizontal U-axis and, in the zig-zag and armchair cases, vertical and horizontal mirror and glide planes, have not been used in band assignation. It is important to complete this task, since it yields many important exact properties of the electronic band structures, some of them being quite independent of the model considered. Let us mention only the band degeneracies, systematic van Hove singularities and the precise selection rules relevant for the processes in nanotubes. Further, some general predictions on the topology of band sticking follow from the interplay between linear and helical quantum numbers, and may be a priori predicted and used for the completely assigned bands.

All the geometrical symmetries of chiral (n_1, n_2), zig-zag $(n, 0)$ and armchair (n, n) SWCT ($\mathcal{C}$, $\mathcal{Z}$ and $\mathcal{A}$ tubes for short) are gathered in the line groups[4] (the factorized and the international notation are given):

$$\boldsymbol{L}_{\mathcal{C}} = \boldsymbol{T}_q^r \boldsymbol{D}_n = \boldsymbol{L} q_p 22, \tag{1a}$$

$$\boldsymbol{L}_{\mathcal{ZA}} = \boldsymbol{T}_{2n}^1 \boldsymbol{D}_{nh} = \boldsymbol{L} 2n_n / mcm. \tag{1b}$$

Here, n is the greatest common divisor of n_1 and n_2, $q = 2(n_1^2+n_1n_2+n_2^2)/n\mathcal{R}$ with $\mathcal{R} = 3$ or $\mathcal{R} = 1$ whether $(n_1 - n_2)/3n$ is integer or not, while the helicity parameters r and p are expressed in terms of n_1 and n_2 by number theoretical functions[5]. The elements of the groups (1) are (the coordinate system and the positions of the symmetry axes and planes are presented in Fig. 1):

$$\ell(t, s, u, v) = (C_q^r | na/q)^t C_n^s U^u \sigma_x^v, \tag{2}$$

where $(C_q^r|na/q)^t$ (Koster-Seitz notation; a is the translational period of the tube) for $t = 0, \pm 1, \ldots$ are the elements of the helical group (screw-axis) $\boldsymbol{T}_q^r$. The rotations C_n^s, $s = 0, \ldots, n-1$, around the z-axis form the subgroup $\boldsymbol{C}_n$. Finally, U is the rotation by π around the x-axis ($u = 0, 1$), and σ_{v} the vertical mirror xz-plane in the case of the achiral tubes, i.e. $v = 0, 1$ for $\mathcal{Z}$ and $\mathcal{A}$ tubes, and $v = 0$ for $\mathcal{C}$ ones. Each carbon atom on the tube is obtained from a single one C_{000} by the action of the element $\ell(t, s, u, 0)$. This enables to enumerate the atoms as C_{tsu}. The isogonal point groups are:

$$\boldsymbol{P}_{\mathcal{C}} = \boldsymbol{D}_q, \quad \boldsymbol{P}_{\mathcal{ZA}} = \boldsymbol{D}_{2nh}. \tag{3}$$

Each electronic eigen state corresponds to the complete set of symmetry based quantum numbers, which singles out an irreducible representation of the symmetry group of SWCT. Knowing this representation the eigen states (in the form of the generalized Bloch functions) and the eigen energies (organized as the energy bands) may be easily found[6,7]. Analysis of the linear and helical symmetry based quantum numbers and their mutual relations is performed in section II; this enable to emphasize *a priori* properties of the band structures, referring to any subsystem (electrons, phonons, etc.). In section III these considerations are further elaborated for the electronic bands: the general dispersion relations are derived and especially in the most usual tight-binding approach the complete symmetry assignation and the Bloch eigen

states are presented. Then, in section IV, possible applications in the analysis of different processes are explained, using the general forms of various tensors (e.g. dielectric permeability, Raman, conductivity) and the selection rules that are given in appendix A. Basic conclusions are reviewed in the last section.

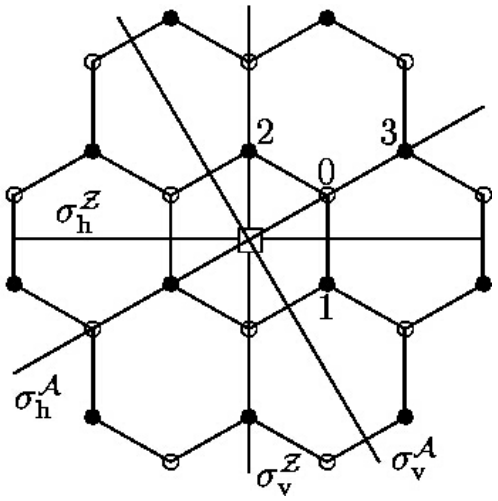

FIG. 1: **Symmetry and neighbors.** Perpendicular to the figure at $\square$ is the U-axis (assumed to be the x-axis), while $\sigma_{\rm h/v}^{\mathcal{Z}/\mathcal{A}}$ stands for vertical and horizontal mirror planes of $\mathcal{Z}$ and $\mathcal{A}$ tubes. Atoms C_{ts0} and C_{ts1} are differed as $\circ$ and $\bullet$. Nearest neighbors of the atom C_{000}, denoted by 0, are the atoms 1, 2 and 3.

II. SYMMETRY AND QUANTUM NUMBERS

For the chiral tubes, there are two sets of quantum numbers used in literature: km- and $\tilde{k}\tilde{m}$-numbers. They correspond to different parameterizations of the irreducible representations[7,8] of the line groups $\mathbf{L}_{\mathcal{C}}$. The inherent physical meaning of the quantum numbers makes one or another choice more suitable for different physical considerations.

The group structure (1a) immediately shows that the conserved quantities[8] are: the helical quasi momentum $\tilde{k}$ related to the screw-axis subgroup $\boldsymbol{T}_q^r$, the z component of the angular quasi momentum $\tilde{m}$ arising from the pure rotational symmetries $\boldsymbol{C}_n$ and the parity with respect to U axis. Note that $\tilde{k}$ includes the linear quasi momentum k and the part of the angular momentum being not included in $\tilde{m}$. The different values of $\tilde{k}$ are within the interval $\widetilde{\rm BZ} = (-\tilde{\pi}/a, \tilde{\pi}/a]$ (here $\tilde{\pi} = \tilde{q}\pi$; $\tilde{q} = q/n$), and $\tilde{m}$ runs over the integers from $(-n/2, n/2]$. As usual, the equality of the quantum numbers modulo these intervals is assumed. The parity quantum number corresponding to the U-axis will be denoted as $+$ and $-$ for even and odd states. Thus, with $\tilde{k}\tilde{m}$-numbers the states are labeled as $|\,\tilde{k}\tilde{m}\rangle$ or $|\,\tilde{k}\tilde{m}\pm\rangle$ for the U-parity even and odd states. Since the U-symmetry reverses the z-components both of the linear and the angular momenta, the state $|\,\tilde{k},\tilde{m}\rangle$ is mapped by U to $|\,-\tilde{k},-\tilde{m}\rangle$, and vice versa. As far as these two states are different, the corresponding energy levels are degenerate, and the doublet spans a two dimensional space carrying the irreducible representation ${}_{\tilde{k}}E_{\tilde{m}}$ with integer $\tilde{m} \in (-n/2, n/2]$. Therefore, it suffices to consider $\tilde{k}$ only in the irreducible domain[6] $\widetilde{\rm ID} = [0, \tilde{\pi}/a]$. Obviously, only if $k = 0, \tilde{\pi}/a$ and $m = 0, n/2$ the states $|\tilde{k},\tilde{m}\rangle$ and $|-\tilde{k},-\tilde{m}\rangle$ are physically the same: $|-\tilde{k},-\tilde{m}\rangle = \pm\,|\tilde{k}\tilde{m}\rangle$. Thus, even or odd states are at the edges[9] of $\widetilde{\rm ID}$: $|00\pm\rangle$, $|\tilde{\pi}0\pm\rangle$, and only for even n also $|\,0, n/2, \pm\rangle$ and $|\,\tilde{\pi}, n/2, \pm\rangle$. These nondegenerate states correspond to the one-dimensional representations ${}_0A_0^{\pm}$, ${}_{\tilde{\pi}}A_0^{\pm}$, ${}_0A_{n/2}^{\pm}$ and ${}_{\tilde{\pi}}A_{n/2}^{\pm}$. So, the eigen energies make at least double degenerate bands over the interior of $\widetilde{\rm ID}$, and only the bands with $m = 0, n/2$ end by even or odd singlet state. As for the other bands, those with the opposite $\tilde{m}$ are sticked together at $\tilde{k} = 0, \tilde{\pi}/a$.

With the km-numbers[7], a state of (quasi)particle propagating along the z-axis with the quasi momentum k and the z-component of the angular momentum m is denoted as $|\,km\rangle$, or $|\,km\pm\rangle$. Reflecting pure translational symmetry, the (linear) quasi momentum k varies within the Brillouin zone ${\rm BZ} = (-\pi/a, \pi/a]$, while m is related to the isogonal rotations and takes on the integer values from $(-q/2, q/2]$, precisely[5] $m = -q/2+1, \ldots, q/2$. It is assumed that the equalities in k and m are modulo these intervals. Since the pure rotation by $2\pi/q$ of the isogonal group (3) is not a symmetry of the system, quantum number m may not be conserved, which is clearly manifested in the selection rules (see the appendix). The states $|\,km\,\rangle$ and $|\,-k,-m\,\rangle$, being mapped one onto another by the U-symmetry, make a degenerate doublet of the irreducible representation ${}_kE_m$ for any k in the interior of the irreducible domain ${\rm ID} = [0, \pi/a]$. At the edge point $k = 0$, when U leaves k invariant, for $m = 1, \ldots, q/2-1$ the state $|\,0m\rangle$ is mapped onto the state $|0,-m\rangle$, yielding again two-dimensional irreducible representations ${}_0E_m$. Only for $m = 0, q/2$ there are nondegenerate even and odd states, $|\,00\pm\rangle$ and $|\,0, q/2, \pm\rangle$, carrying the one-dimensional irreducible representations ${}_0A_0^{\pm}$ and ${}_0A_{q/2}^{\pm}$. At $k = \pi/a$, U intertwins the states $|\,\pi m\rangle$ and $|\,\pi m'\rangle$, where $m' = -p-m$. Thus, the singlets[9] $|\,\pi, -p/2, \pm\rangle$ and $|\,\pi, (q-p)/2, \pm\rangle$ appear only for p even[5] and correspond to the one-dimensional representations ${}_{\pi}A_{-p/2}^{\pm}$ and ${}_{\pi}A_{(q-p)/2}^{\pm}$. The remaining integers $m \in (-p/2, (q-p)/2)$ give the double degenerate levels of the representations ${}_{\pi}E_m$. Consequently, the bands with m and m', differ in the interior of ID, but they stick together at $k = \pi/a$ as well as those with opposite $m \neq 0, q/2$ are sticked together at $k = 0$.

The additional mirror planes $\sigma_{\rm v}$ and $\sigma_{\rm h} = U\sigma_{\rm v}$ yield new parities in the cases of $\mathcal{Z}$ and $\mathcal{A}$ tubes. Even and odd states with respect to $\sigma_{\rm v}$ are labeled by A and B. The parity of the horizontal mirror plane $\sigma_{\rm h}$ is denoted

as that of U, i.e. '+' and '−' now points to the even and odd states with respect to either one of these z-reversing operations. Obviously, $\sigma_{\rm v}$ leaves k invariant and m is reversed[10]. Therefore, in the interior of the ID, the U-degenerate states $|km\rangle$ and $|-k,-m\rangle$ are mapped by $\sigma_{\rm v}$ onto $|k,-m\rangle$ and $|-k,m\rangle$. For each $m=1,\ldots,n-1$ all these states span the four-dimensional irreducible representation ${}_kG_m$ of the four fold degenerate band. Only for $m=0,n$ the degeneracy remains two fold, in accordance with the two dimensional irreducible representations ${}_kE_0^{A/B}$ and ${}_kE_n^{A/B}$ over $\sigma_{\rm v}$-even or odd states $|km,A/B\rangle$ and $|-km,A/B\rangle$. If further $k=0$, the states $|\,00,\pm,A/B\rangle$ and $|\,0n,\pm,A/B\rangle$ are nondegenerate, corresponding to the one-dimensional representations ${}_0A_0^{\pm}$, ${}_0B_0^{\pm}$, ${}_0A_n^{\pm}$ and ${}_0B_n^{\pm}$. For the remaining $m=1,\ldots,n-1$, the states $|\,0m\pm\rangle$ and $|\,0,-m\pm\rangle$ are degenerate giving two-dimensional representations ${}_0E_m^{\pm}$ (parity with respect to $\sigma_{\rm h}$). At the other ID edge $k=\pi/a$, for integer $m\in(0,n/2)$ the four-fold degenerate states $|\pi m\rangle$, $|\,\pi,-m\rangle$, $|\,\pi,n-m\rangle$ and $|\,\pi,m-n\rangle$ span the representation ${}_\pi G_m$. As for $m=0,n$, the states $|\,\pi 0,A/B\rangle$ and $|\,\pi n,A/B\rangle$ as well as the states (existing only for n even) $|\pi,n/2,\pm\rangle$ and $|\pi,-n/2,\pm\rangle$ are degenerate, being associated to the representations ${}_\pi E_0^A$, ${}_\pi E_0^B$ and ${}_\pi E_{n/2}^{\pm}$.

In terms of energies only, one concludes that the systematic band degeneracy is caused by the parities only. Their nontrivial action on the momenta eigen states defines the irreducible representations of the symmetry group (1) of the dimension 1 (representations A and B), 2 (E) or 4 (G), uniquely corresponding to each complete set of all quantum numbers. The U-axis is manifested as the symmetry of the bands with respect to $\tilde{k}=0,q\pi/na$:

$$\epsilon_{\tilde{m}}(\tilde{k})=\epsilon_{-\tilde{m}}(-\tilde{k})=\epsilon_{-\tilde{m}}(2\tilde{\pi}/a-\tilde{k}), \tag{4a}$$

$$\epsilon_{\tilde{m}}(\tilde{\pi}/a-\tilde{k})=\epsilon_{-\tilde{m}}(\tilde{\pi}/a+\tilde{k}). \tag{4b}$$

Two consequences, the possibility to consider only the irreducible domain and the obligate double degeneracy in its interior have been emphasized already. In addition, some general topological properties of the bands can be predicted. The conditions (4) at $\tilde{k}=0,\tilde{\pi}/a$ show that $\tilde{m}$ and $-\tilde{m}$ bands are sticked together in the both $\widetilde{\rm ID}$ edges. These results in the terms of km numbers[10] become the bands $\pm m$ are sticked together at $k=0$, as well as the bands m and $m+p$ at π/a. Altogether, the irreducible domain $\widetilde{\rm ID}$ contains q/n segments as wide as ID; the part of a $\tilde{k}\tilde{m}$ band over each of the segments is one of the km bands having the quantum number $m=\tilde{m}+jn$ ($j=0,\ldots,\tilde{q}-1$). The successive segments correspond to the sticked together km bands. Further, the relations (4) imply van Hove singularities at $\tilde{k}=0,\tilde{\pi}/a$ of the $\tilde{m}=0,n$ bands (when $\tilde{m}=-\tilde{m}$): $[{\rm d}\epsilon_{\tilde{m}}(\tilde{k})/{\rm d}\tilde{k}]_{\tilde{k}=0,\tilde{\pi}/a}=0$. The same singularities[10] are found for $m=0,q/2$ at $k=0$ and $m=-p/2,(q-p)/2$ at $k=\pi/a$. The importance of the coincidence of these singularities with the U-parity even and odd states will be discussed later on. Additional mirror planes of the achiral tubes force m and $-m$ bands to coincide, causing additional degeneracy, together with the condition

$$\epsilon_{\tilde{m}}(\tilde{k})=\epsilon_{\tilde{m}}(-\tilde{k})=\epsilon_{\tilde{m}}(2\tilde{\pi}/a-\tilde{k}). \tag{5}$$

This yields the z-reversal parity of all the states at $k=0$ and $m=n/2$ states at $k=\pi/a$, as well as in the corresponding van Hove singularities. All these general conclusions are transparently verified by the tight-binding electronic bands given in Fig. 2. For example, all the bands of the achiral tubes have extremes at $k=0$ and only $m=5$ band also in $k=\pi/a$. Of course, besides these systematic z-reversal parities caused extremes, other ones may appear[11] depending on the considered model.

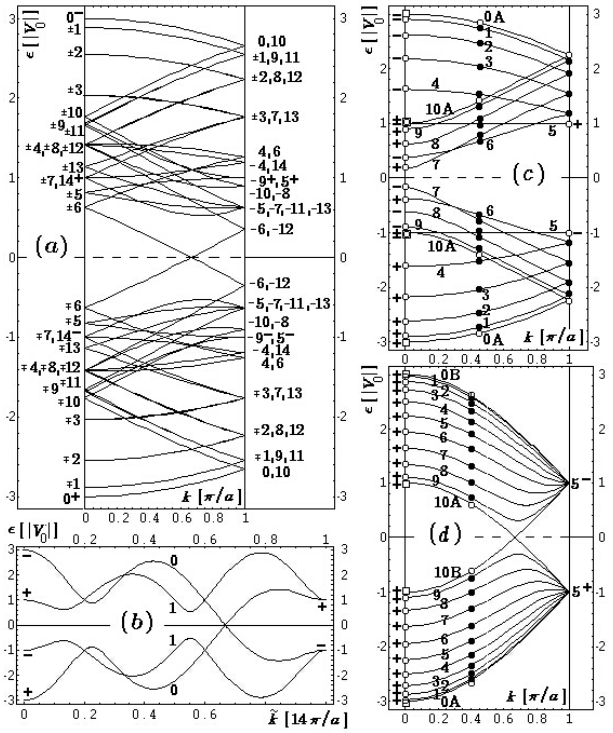

FIG. 2: **Symmetry assigned electronic bands of SWCT**. For the chiral tube $(8,2)$ (line group $\boldsymbol{T}_{28}^{11}\mathbf{D}_2=\boldsymbol{L}28_{18}22$, $a=\sqrt{7}a_0=6.5$Å) the bands are double degenerate in the interior of ID, while at the edges the U-parity singlets are emphasized by + or −; km- (m is given at both edges of the band ${}_kE_m$) and $\tilde{k}\tilde{m}$-numbers assignation on (a) and (b). (c) and (d): The bands of the zig-zag $(10,0)$ and the armchair $(10,10)$ tubes (line group $\boldsymbol{T}_{20}^{1}\boldsymbol{D}_{10h}=\mathbf{L}20_{10}/mcm$, $a_{\mathcal{Z}}=\sqrt{3}a_0=4.26$Å, and $a_{\mathcal{A}}=a_0$) are either four-fold (${}_kG_m$, •) or double degenerate (${}_kE_{0/10}^{A/B}$, ∘, $\sigma_{\rm v}$ parity A or B given next to m); z-reversal parity (+ or −) and nondegenerate states (box) appear at the edges of ID.

Let us remark that the same quantum numbers may characterize several, say N (frequency number[6] of the

corresponding representation) eigen states with equal or different eigen energies. In such cases the index F differing between such states is added. For example, for each m there are $N = 2\ {}_kE_m$ electronic bands of $\mathcal{C}$-tubes (section III). These eigen energies $\epsilon_m^{\pm}(k)$ and the vectors $|\,km;\pm\rangle$, $|\,{-k},{-m};\pm\rangle$ are distinguished by $F = \pm$.

III. ELECTRONIC π-BANDS

The tight binding hamiltonian including a single π-orbital $|\,tsu\rangle$ per site C_{tsu} is

$$H = \sum_{tsu}\sum_{t's'u'} H_{tsu,t's'u'}\ |\,tsu\rangle\langle t's'u'\,|\ .$$

The electronic band structure for such a hamiltonian has been calculated (regarding nearest neighbor interactions) with the help of the translational and the principle axis rotational symmetries. The resulting assignation thus involved either km or $\tilde{k}\tilde{m}$-numbers[2,3]. Here we complete the assignation by the additional parities of the full symmetry group. The results are obtained applying the modified group projector technique[7].

Depending on the choice of the quantum numbers it is convenient to introduce the phases:

$$\begin{aligned}\psi_m^k(t,s) &= \tfrac{kan+2\pi mr}{q}t + \tfrac{2\pi m}{n}s,\\ \tilde{\psi}_{\tilde{m}}^{\tilde{k}}(t,s) &= \tfrac{\tilde{k}a}{\tilde{q}}t + \tfrac{2\pi\tilde{m}}{n}s.\end{aligned} \tag{6}$$

Then, for the generic bands of the chiral tube (double degenerate ${}_kE_m$ or ${}_{\tilde{k}}E_{\tilde{m}}$ bands for any allowed m or $\tilde{m}$ along the interior of the irreducible domain) the dispersion relations and the corresponding eigen vectors are obtained solving the eigen problem of

$$H_m(k) = \begin{pmatrix} h_m^0(k) & h_m^{1*}(k)\\ h_m^1(k) & h_m^0(k)\end{pmatrix}, \tag{7a}$$

$$h_m^u(k) = \sum_{ts} H_{tsu}\mathrm{e}^{\mathrm{i}\psi_k^m(t,s)} \quad (u=0,1), \tag{7b}$$

with $H_{tsu} = H_{000,tsu}$. Finally, for each m one finds two bands

$$\epsilon_m^{\pm}(k) = h_m^0(k) \pm |h_m^1(k)| \tag{8a}$$

with the corresponding generalized Bloch eigen functions

$$|\,km;\pm\rangle = \sum_{ts}\mathrm{e}^{-\mathrm{i}\psi_m^k(t,s)}\big(\,|\,ts0\rangle \pm \mathrm{e}^{\mathrm{i}h_m^k}\,|\,ts1\rangle\big), \tag{8b}$$

$$|\,{-k},{-m};\pm\rangle = \sum_{ts}\mathrm{e}^{\mathrm{i}\psi_m^k(t,s)}\big(\,|\,ts1\rangle \pm \mathrm{e}^{\mathrm{i}h_m^k}\,|\,ts0\rangle\big), \tag{8c}$$

where $h_m^k = \mathrm{Arg}\big(h_m^1(k)\big)$. To get the expressions in terms of $\tilde{k}\tilde{m}$ quantum numbers the angles $\tilde{\psi}_{\tilde{m}}^{\tilde{k}}(t,s)$ are used to define $\tilde{h}_{\tilde{m}}^u(\tilde{k})$ and $\tilde{h}_{\tilde{m}}^{\tilde{k}}$ in the same way.

Note that the atoms with $u = 0$ and $u = 1$ contribute only to the diagonal and off diagonal terms of $H_m(k)$, respectively. Consequently, in the dispersion relations (8a), the interactions of C_{000} with C_{ts0} atoms determine for each k the average energy of two bands, while the interactions with C_{ts1} atoms shifts up and down symmetrically this average to the eigen energies. Within $\pi^{\perp}$-orbitals tight-binding approximation this result is obviously not restricted to some of the neighbors and includes the local distortions induced by the cylindrical geometry. Further, note that $H_{tsu,t's'u'}$ would be equal to $\langle tsu\ |\ H\ |\ t's'u'\rangle$ if and only if the atomic orbitals $|\,tsu\rangle$ were orthonormal basis. Since expressed in terms of $H_{tsu,t's'u'}$ matrix elements, equations (8) refer to the realistic nonorthonormal case (therefore the resulting Bloch functions are not orthonormalized). To take advantage of the calculated[12] elements $\langle tsu\ |\ H\ |\ t's'u'\,\rangle$ and the overlap integrals $\langle 000\,|\,tsu\,\rangle$ one uses another matrix having also the form (7), but with $\langle 000\,|\,H\,|tsu\rangle$ instead of H_{tsu}. Multiplying (7a) by the inverse of the analogous matrix of the overlap integrals, one gets $H_m(k)$ completely in terms of the known Slater-Koster elements and the overlap integrals.

Also, the resultgiven in (8a) is general in the sense that the eigen energies at the edges of the irreducible domain can be obtained from this expression by substituting the limiting values of km (or $\tilde{k}\tilde{m}$) numbers; the nondegenerate ones point out the states with U-parity. For the $\mathcal{Z}$ and $\mathcal{A}$ tubes the dispersion relations can be derived, too: only $n_1 = q/2 = n$ and $n_2 = 0$ for the zig-zag or $n_1 = n_2 = n$ for the armchair tubes should be used. In these cases (8a) is the same for m and $-m$, reflecting the anticipated general conclusion that the bands of the achiral tubes are four-fold degenerate apart from the double degenerate $m = 0, n$ bands. These double degenerate bands are with even σ_{v}-parity for $\mathcal{Z}$ tubes, while they form two pairs with opposite σ_{v} parity in $\mathcal{A}$ tubes. Nevertheless, the symmetry adapted basis for the four-fold degenerate bands and the representations with parities cannot be such straightforwardly derived from (8c), and each of these representation should be considered separately.

As for the most usual orthogonal orbitals nearest neighbors approximation, the sums in (7) are restricted to the constant term H_{000} in $h_m^0(k)$ and to the three nearest neighbors in $h_m^1(k)$. Taking $H_{000} = 0$, i.e. shifting the energy scale for H_{000}, and substituting in (6) for the nearest neighbors (Fig. 1) the parameters

$$\begin{aligned} t_1 &= -\frac{n_2}{n}, \quad s_1 = \frac{2n_1 + (1+r\mathcal{R})n_2}{q\mathcal{R}},\\ t_2 &= \frac{n_1}{n}, \quad s_2 = \frac{(1-r\mathcal{R})n_1 + 2n_2}{q\mathcal{R}},\\ t_3 &= t_1 + t_2, \quad s_3 = s_1 + s_2,\end{aligned}$$

one gets pairs of equally assigned double degenerate generic bands for each allowed m (i.e. $\tilde{m}$):

$$\epsilon_{E_m}^{\pm}(k) = \pm|\sum_{i=1}^{3} H_{t_is_i1}\mathrm{e}^{\mathrm{i}\psi_m^k(t_i,s_i)}|. \tag{9}$$

As usual, the same expression but with $\psi_{\tilde{m}}^{\tilde{k}}(t_i,s_i)$ gives

the bands $\epsilon^{\pm}_{E_{\tilde{m}}}(\tilde{k})$ assigned by $\tilde{k}\tilde{m}$-numbers.

TABLE I: **Bands and symmetry-adapted eigen vectors of the carbon nanotubes.** For each irreducible representation the corresponding frequency number N, energy ϵ in the simplest (orthogonal orbitals, nearest neighbors, homogeneous distortions) model and generalized Bloch functions $\mid km\Pi\,\rangle$ of the corresponding bands are given. Substituting ψ^k_m and h^k_m by $\tilde{\psi}^{\tilde{k}}_{\tilde{m}}$ and $\tilde{h}^{\tilde{k}}_{\tilde{m}}$ one obtains these quantities in $\tilde{k}\tilde{m}$ numbers (see (6) and (7) and the comment bellow). $\gamma = \mathrm{Arg}(1+2\mathrm{e}^{\mathrm{i}\frac{ka}{2}}\cos\frac{\pi m}{n})$.

$\mathcal{C}$	N	ϵ	Generalized Bloch functions
${}_0A^{\Pi}_m$	1	$V\Pi(1+2\mathrm{e}^{2\mathrm{i}\frac{m\pi}{q}})$	$\|0m\Pi\rangle = \frac{1}{\sqrt{\|\boldsymbol{L}_{\mathcal{C}}\|}}\sum_{ts}\mathrm{e}^{-\mathrm{i}\psi^0_m(t,s)}(\|ts0\rangle + \Pi\,\|ts1\rangle)$
${}_\pi A^{\Pi}_m$	1	$-V\Pi$	$\|\pi m\Pi\rangle = \frac{1}{\sqrt{\|\boldsymbol{L}_{\mathcal{C}}\|}}\sum_{ts}\mathrm{e}^{-\mathrm{i}\psi^\pi_m(t,s)}(\|ts0\rangle + \Pi\,\|ts1\rangle)$
${}_kE_m$	2	$\pm\|V\sum_i \mathrm{e}^{\mathrm{i}\psi^k_m(t_i,s_i)}\|$	$\|km;\pm\rangle = \frac{1}{\sqrt{\|\boldsymbol{L}_{\mathcal{C}}\|}}\sum_{ts}\mathrm{e}^{-\mathrm{i}\psi^k_m(t,s)}(\|ts0\rangle \pm \mathrm{e}^{\mathrm{i}h^k_m}\,\|ts1\rangle)$
			$\|-k,-m;\pm\rangle = \frac{1}{\sqrt{\|\boldsymbol{L}_{\mathcal{C}}\|}}\sum_{ts}\mathrm{e}^{\mathrm{i}\psi^k_m(t,s)}(\|ts1\rangle \pm \mathrm{e}^{\mathrm{i}h^k_m}\,\|ts0\rangle)$
$\mathcal{Z}$	N	ϵ	Generalized Bloch functions
${}_0A^{\Pi}_m$	1	$V\Pi(1+2\mathrm{e}^{\mathrm{i}\frac{m\pi}{n}})$	$\|0m\Pi A\rangle = \sqrt{\frac{2}{\|\boldsymbol{L}_{\mathcal{Z}}\|}}\sum_{ts}\mathrm{e}^{-\mathrm{i}\frac{m\pi}{n}t}(\|ts0\rangle + \Pi\,\|ts1\rangle)$
${}_0E^{\Pi}_m$	1	$V\Pi(1+2\cos\frac{m\pi}{n})$	$\|0m\Pi\rangle = \sqrt{\frac{2}{\|\boldsymbol{L}_{\mathcal{Z}}\|}}\sum_{ts}\mathrm{e}^{-\mathrm{i}\frac{m\pi}{n}(2s+t)}(\|ts0\rangle + \Pi\mathrm{e}^{\mathrm{i}\frac{2m\pi}{n}}\,\|ts1\rangle)$
			$\|0,-m,\Pi\rangle = \sqrt{\frac{2}{\|\boldsymbol{L}_{\mathcal{Z}}\|}}\sum_{ts}\mathrm{e}^{\mathrm{i}\frac{m\pi}{n}(2s+t)}(\mathrm{e}^{\mathrm{i}\frac{2m\pi}{n}}\,\|ts0\rangle + \Pi\,\|ts1\rangle)$
${}_kE^{A}_m$	2	$\pm\|V\|\sqrt{5+4\mathrm{e}^{\mathrm{i}\frac{m\pi}{n}}\cos\frac{ka}{2}}$	$\|kmA;\pm\rangle = \sqrt{\frac{2}{\|\boldsymbol{L}_{\mathcal{Z}}\|}}\sum_{ts}\mathrm{e}^{-\mathrm{i}(\frac{m\pi}{n}+\frac{ka}{2})t}(\|ts0\rangle \pm \mathrm{e}^{\mathrm{i}h^m_k}\,\|ts1\rangle)$
			$\|-k,m,A;\pm\rangle = \sqrt{\frac{2}{\|\boldsymbol{L}_{\mathcal{Z}}\|}}\sum_{ts}\mathrm{e}^{-\mathrm{i}(\frac{m\pi}{n}-\frac{ka}{2})t}(\|ts1\rangle \pm \mathrm{e}^{\mathrm{i}h^m_k}\,\|ts0\rangle)$
${}_\pi E^{\Pi}_{\frac{n}{2}}$	1	$-V\Pi$	$\|\pi,\frac{n}{2},\Pi\rangle = \sqrt{\frac{2}{\|\boldsymbol{L}_{\mathcal{Z}}\|}}\sum_{ts}(-1)^{s+t}(\|ts0\rangle + \Pi\,\|ts1\rangle)$
			$\|\pi,-\frac{n}{2},\Pi\rangle = \sqrt{\frac{2}{\|\boldsymbol{L}_{\mathcal{Z}}\|}}\sum_{ts}(-1)^{s}(\|ts0\rangle + \Pi\,\|ts1\rangle)$
${}_kG_m$	2	$\pm V\sqrt{1+4\cos\frac{ka}{2}\cos\frac{m\pi}{n}+4\cos^2\frac{m\pi}{n}}$	$\|km;\pm\rangle = \sqrt{\frac{2}{\|\boldsymbol{L}_{\mathcal{Z}}\|}}\sum_{ts}\mathrm{e}^{-\mathrm{i}\frac{ka}{2}t}\mathrm{e}^{-\mathrm{i}\frac{m\pi}{n}(t+2s)}(\|ts0\rangle \pm \mathrm{e}^{\mathrm{i}\gamma}\mathrm{e}^{\mathrm{i}\frac{2m\pi}{n}}\,\|ts1\rangle)$
			$\|k,-m;\pm\rangle = \sqrt{\frac{2}{\|\boldsymbol{L}_{\mathcal{Z}}\|}}\sum_{ts}\mathrm{e}^{-\mathrm{i}\frac{ka}{2}t}\mathrm{e}^{\mathrm{i}\frac{m\pi}{n}(t+2s)}(\mathrm{e}^{\mathrm{i}\frac{2m\pi}{n}}\,\|ts0\rangle \pm \mathrm{e}^{\mathrm{i}\gamma}\,\|ts1\rangle)$
			$\|-k,m;\pm\rangle = \sqrt{\frac{2}{\|\boldsymbol{L}_{\mathcal{Z}}\|}}\sum_{ts}\mathrm{e}^{\mathrm{i}\frac{ka}{2}t}\mathrm{e}^{-\mathrm{i}\frac{m\pi}{n}(t+2s)}(\mathrm{e}^{\mathrm{i}\frac{2m\pi}{n}}\,\|ts1\rangle \pm \mathrm{e}^{\mathrm{i}\gamma}\,\|ts0\rangle)$
			$\|-k,-m;\pm\rangle = \sqrt{\frac{2}{\|\boldsymbol{L}_{\mathcal{Z}}\|}}\sum_{ts}\mathrm{e}^{\mathrm{i}\frac{ka}{2}t}\mathrm{e}^{\mathrm{i}\frac{m\pi}{n}(t+2s)}(\|ts1\rangle \pm \mathrm{e}^{\mathrm{i}\gamma}\mathrm{e}^{\mathrm{i}\frac{2m\pi}{n}}\,\|ts0\rangle)$
$\mathcal{A}$	N	ϵ	Generalized Bloch functions
${}_0\Pi^{+}_m$	1	$V\Pi(1+2\mathrm{e}^{\mathrm{i}\frac{m\pi}{n}})$	$\|0m+\Pi\rangle = \sqrt{\frac{2}{\|\boldsymbol{L}_{\mathcal{A}}\|}}\sum_{ts}\mathrm{e}^{-\mathrm{i}\frac{m\pi}{n}t}(\|ts0\rangle + \Pi\,\|ts1\rangle)$
${}_0E^{+}_m$	2	$\pm\|V\|\sqrt{5+4\cos\frac{m\pi}{n}}$	$\|0m+;\pm\rangle = \sqrt{\frac{2}{\|\boldsymbol{L}_{\mathcal{A}}\|}}\sum_{ts}\mathrm{e}^{-\mathrm{i}\frac{m\pi}{n}(2s+t)}(\|ts0\rangle \pm \mathrm{e}^{\mathrm{i}h^m_0}\,\|ts1\rangle)$
			$\|0,-m,+;\pm\rangle = \sqrt{\frac{2}{\|\boldsymbol{L}_{\mathcal{A}}\|}}\sum_{ts}\mathrm{e}^{\mathrm{i}\frac{m\pi}{n}(2s+t)}(\|ts1\rangle \pm \mathrm{e}^{\mathrm{i}h^m_0}\,\|ts0\rangle)$
${}_kE^{\Pi}_m$	1	$V\Pi(1+2\mathrm{e}^{\mathrm{i}\frac{m\pi}{n}}\cos\frac{ka}{2})$	$\|km\Pi\rangle = \sqrt{\frac{2}{\|\boldsymbol{L}_{\mathcal{A}}\|}}\sum_{ts}\mathrm{e}^{-\mathrm{i}(\frac{m\pi}{n}+\frac{ka}{2})t}(\|ts0\rangle + \Pi\,\|ts1\rangle)$
			$\|-k,m,\Pi\rangle = \sqrt{\frac{2}{\|\boldsymbol{L}_{\mathcal{A}}\|}}\sum_{ts}\mathrm{e}^{-\mathrm{i}(\frac{m\pi}{n}-\frac{ka}{2})t}(\|ts0\rangle + \Pi\,\|ts1\rangle)$
${}_\pi E^{\Pi}_{\frac{n}{2}}$	1	$-V\Pi$	$\|\pi,\frac{n}{2},\Pi\rangle = \sqrt{\frac{2}{\|\boldsymbol{L}_{\mathcal{A}}\|}}\sum_{ts}(-1)^{s+t}(\|ts0\rangle + \Pi\,\|ts1\rangle)$
			$\|\pi,-\frac{n}{2},\Pi\rangle = \sqrt{\frac{2}{\|\boldsymbol{L}_{\mathcal{A}}\|}}\sum_{ts}(-1)^{s}(\Pi\,\|ts0\rangle + \|ts1\rangle)$
${}_kG_m$	2	$\pm V\sqrt{1+4\cos\frac{ka}{2}\cos\frac{m\pi}{n}+4\cos^2\frac{ka}{2}}$	$\|km;\pm\rangle = \sqrt{\frac{2}{\|\boldsymbol{L}_{\mathcal{A}}\|}}\sum_{ts}\mathrm{e}^{-\mathrm{i}\frac{ka}{2}t}\mathrm{e}^{-\mathrm{i}\frac{m\pi}{n}(t+2s)}(\|ts0\rangle \pm \mathrm{e}^{\mathrm{i}h^m_k}\,\|ts1\rangle)$
			$\|k,-m;\pm\rangle = \sqrt{\frac{2}{\|\boldsymbol{L}_{\mathcal{A}}\|}}\sum_{ts}\mathrm{e}^{-\mathrm{i}\frac{ka}{2}t}\mathrm{e}^{\mathrm{i}\frac{m\pi}{n}(t+2s)}(\|ts1\rangle \pm \mathrm{e}^{\mathrm{i}h^m_k}\,\|ts0\rangle)$
			$\|-k,m;\pm\rangle = \sqrt{\frac{2}{\|\boldsymbol{L}_{\mathcal{A}}\|}}\sum_{ts}\mathrm{e}^{\mathrm{i}\frac{ka}{2}t}\mathrm{e}^{-\mathrm{i}\frac{m\pi}{n}(t+2s)}(\|ts0\rangle \pm \mathrm{e}^{\mathrm{i}h^m_k}\,\|ts1\rangle)$
			$\|-k,-m;\pm\rangle = \sqrt{\frac{2}{\|\boldsymbol{L}_{\mathcal{A}}\|}}\sum_{ts}\mathrm{e}^{\mathrm{i}\frac{ka}{2}t}\mathrm{e}^{\mathrm{i}\frac{m\pi}{n}(t+2s)}(\|ts1\rangle \pm \mathrm{e}^{\mathrm{i}h^m_k}\,\|ts0\rangle)$

Finally, the rolling up induced differences in the interatomic distances of the honeycomb lattice are frequently neglected (homogeneous distortions approximation), which is achieved by setting $H_{t_i s_{i1}} = V$ for the nearest neighbors (V is estimated between -3.003 eV and -2.5 eV). All the dispersion relations and the corresponding eigen states (in the form of generalized Bloch sums) are given in the Table I for this approximation, and in Fig. 2 the assignation of these bands for several tubes is presented.

IV. SELECTION RULES

One of the most important benefits from the assignation by all quantum numbers comes through the applications of the selection rules in various calculations of physical properties of nanotubes. As it was shown in the section II, each allowed pair of numbers (k, m) or $(\tilde{k}, \tilde{m})$, together with the parities when necessary, singles out states corresponding to one irreducible representation. In this sense, a representation is specified by $(km\Pi)$, where Π stands for all possible parities. If the representation is degenerate the "raw" index r running from 1 to the dimension of the representation is used to enumerate the states of the same irreducible subspace (with the same eigen energy). Altogether, the state is denoted as $|km\Pi r; F\rangle$. For example, the symmetry adapted eigen states of the ${}_kE_m$ electronic bands of $\mathcal{C}$-tubes (section III) are now denoted as $|\, km1; \pm\rangle = |\, km; \pm\rangle$ and $|km2; \pm\rangle = |-k, -m; \pm\rangle$. Also the components $Q_r^{(km\Pi)}$ of the physical tensor Q are associated to the same quantum numbers (i.e. irreducible representations), giving their transformation rules under the line group symmetry operations. Then, the matrix elements of Q are expressed in the Wigner-Eckart form[13]:

$$\langle\!\langle k_f m_f \Pi_f r_f; F_f \mid Q_r^{(km\Pi)} \mid k_i m_i \Pi_i r_i; F_i\rangle = \langle k_f m_f \Pi_f r_f \mid km\Pi, r; k_i m_i \Pi_i r_i \rangle Q(k_f m_f \Pi_f; F_f \| km\Pi \| k_i m_i \Pi_i; F_i). \quad (10)$$

Here, $Q(k_f m_f \Pi_f; F_f \| km\Pi \| k_i m_i \Pi_i; F_i)$, the reduced matrix element, is independent on the indices r, r_i and r_f. The Clebsch-Gordan coefficients $\langle k_f m_f \Pi_f r_f \mid km\Pi r; k_i m_i \Pi_i r_i \rangle$, being independent on Q, are *a priori* given by the symmetry of the system; the matrix elements are thus subjected to the selection rules showing when these coefficients are nonzero.

The Clebsch-Gordan coefficients comprise complete information on the selection rules. For the SWCT symmetry groups (1) they are given in the appendix. Generally they reflect conservation laws of the linear momentum $\Delta k = k_f - k_i \doteq k$, helical momentum $\Delta\tilde{k} = \tilde{k}_f - \tilde{k}_i \doteq \tilde{k}$, pure angular momentum $\Delta\tilde{m} = \tilde{m}_f - \tilde{m}_i \doteq \tilde{m}$ and parities $\Pi_f = \Pi\Pi_i$ (assuming $+1$ for "$+$" or A, and -1 for "$-$" and B). The z component of the total quasi angular momentum is not conserved since $\Delta m = m_f - m_i \doteq m + Kp$ and Kp may not be a multiple of q. In fact, among the isogonal rotations C_q^s only the C_n^s are symmetries of nanotubes, and the corresponding $\tilde{m}$ is conserved, since p is a multiple of n. This is important in the Umklapp processes, when K is non-vanishing and m is changed.

The symmetry properties of the most interesting tensors are expressed[14] in terms of the three dimensional vector representations D^p and D^a (polar and axial) of $\boldsymbol{L}$, since these tensors are functions of the radius vector $\boldsymbol{r}$, momentum $\boldsymbol{p}$, electrical field $\boldsymbol{E}$ (polar vectors), angular momentum $\boldsymbol{l}$ and magnetic field $\boldsymbol{H}$ (axial vectors). The irreducible components of the corresponding representations are given in the Table II. For all of them $k = 0$, causing that only direct processes are encountered and now m is also a conserved quantum number (since $k_i = k_f$ yields $K = 0$). This means that their symmetry properties are related to the isogonal groups (3).

To facilitate the application of (10) we discuss the general forms of some of the tensors indicated in a Table II being related to the optical properties[15] of nanotubes.

In the linear approximation the tensor of the dielectric permeability in the weak external electric field $\boldsymbol{E}$ is $\varepsilon_{[ij]}(\boldsymbol{E}) = \varepsilon_{[ij]}(0) + \sum_k \alpha_{[ij]k}\boldsymbol{E}_k$. For the chiral tubes, the general form of the zero field permeability tensor[4] is $\varepsilon(0) = \mathrm{diag}(\varepsilon_{xx}, \varepsilon_{xx}, \varepsilon_{zz})$. As the frequency number of the trivial representation ${}_0A_0^+$ in the $\alpha_{[ij]k}$ is equal to one, the single parameter α, determined by the tube microscopic properties, controls the field-dependent dielectric permeability behaviour: $\varepsilon(\boldsymbol{E}) = \begin{pmatrix} \varepsilon_{xx} & 0 & \alpha E_y \\ 0 & \varepsilon_{xx} & -\alpha E_x \\ \alpha E_y & -\alpha E_x & \varepsilon_{zz} \end{pmatrix}$. Thus, the optical activity of $\mathcal{C}$ tubes is changed by the perpendicular electric field, and instead of one there are two optic axes whose direction depend on the applied field. For the $\mathcal{Z}$ and $\mathcal{A}$ tubes the external field does not change their optical *symmetry*, since no trivial component appears in the decomposition.

The electromagnetic response to a weak applied field is characterized by the dielectric function $\varepsilon_{ij}(\boldsymbol{k}, \omega)$. Although optical absorption and diffraction are well described within the long-wavelength limit, for the optical activity the terms of ε_{ij} linear in the components of the wave vector $\boldsymbol{k}$ (having different symmetry from the $\boldsymbol{k}$-independent ones) should be considered. These linear terms define the tensor γ_{ijk} and its symmetric and antisymmetric[16] parts with respect to the last two subscripts: $\gamma_{ijk} = [\partial\varepsilon_{ij}(\boldsymbol{k}, \omega)/\partial k_l]_{\boldsymbol{k}=0} = \mathrm{i}(\gamma^A_{i\{jl\}} + \gamma^S_{i[jl]})$. For the $\mathcal{Z}$ and $\mathcal{A}$ tubes there is no linear optical response while for the chiral tubes the antisymmetric part $\gamma^A_{i\{jl\}}$ is determined by two independent parameters involved in six nonvanishing tensor elements: $\gamma^A_{xyz} = \gamma^A_{yzx} =$

$-\gamma^A_{xzy} = -\gamma^A_{yxz}$ are related to the interband transitions ${}_0A^{\pm}_0 \leftrightarrow {}_0E_1$, ${}_kE_m \leftrightarrow {}_kE_{m+1}$ ($k \in [0,\pi]$), ${}_0A_{q/2} \leftrightarrow {}_0E_{q/2-1}$ (this follows from (10) when the operators p_x, p_y, l_x and l_y are substituted for Q), while $\gamma^A_{zxy} = -\gamma^A_{zyx}$ are related to the interband transitions ${}_0A^{\pm}_0 \leftrightarrow {}_0A^{\mp}_0$ and ${}_0A^{\pm}_{q/2} \leftrightarrow {}_0A^{\mp}_{q/2}$ (now p_z and l_z are used). The single independent parameter of $\gamma^S_{i[jl]}$ is involved in the four nonvanishing tensor elements: $\gamma^S_{xyz} = \gamma^S_{xzy} = -\gamma^S_{yxz} = -\gamma^S_{yzx}$ related to the interband transitions induced by the symmetric operator $\frac{1}{2}(\hat{z}\hat{p}_y + \hat{y}\hat{p}_z + H.c.)$.

The conductivity tensor σ_{ij} of a system in a sufficiently weak magnetic field $\boldsymbol{H}$ is well approximated quadratically:

$$\sigma_{ij}(\boldsymbol{H}) = \sigma_{[ij]}(0) + \sum_{k=1}^{3} \rho_{\{ij\}k} H_k + \sum_{k=1}^{3}\sum_{l=1}^{3} \beta_{[ij][kl]} H_k H_l,$$

where the symmetry[4,17] allows a symmetric tensor $\sigma_{[ij]}(0) = \mathrm{diag}(\sigma_{xx}, \sigma_{xx}, \sigma_{zz})$. The 3rd rank tensor $\rho_{\{ij\}k}$ is responsible for the linear contribution of the field (Hall effect), while the 4th rank tensor $\beta_{[ij][kl]}$ introduces a small correction to the main effect. Because of the symmetry, $\rho_{\{ij\}k}$ is of the same form for all SWCT ($\mathcal{C}, \mathcal{Z}, \mathcal{A}$): two independent parameters ρ_1 and ρ_2 define its six nonvanishing tensor components: $\rho_{xyz} = -\rho_{yxz} = \rho_1$, $\rho_{xzy} = -\rho_{zxy} = \rho_{zyx} = -\rho_{zxy} = \rho_2$. Also $\beta_{[ij][kl]}$ is of the same form for the chiral and the achiral SWCT, with six independent parameters involved within altogether 21 nonzero components: $\beta_{xxxx} = \beta_{yyyy} = \beta_1$, $\beta_{zzzz} = \beta_2$, $\beta_{xxyy} = \beta_{yyxx} = \beta_3$ $\beta_{xyxy} = \beta_{xyyx} = \beta_{yxxy} = \beta_{yxyx} = \frac{1}{2}(\beta_1 - \beta_3)$, $\beta_{xxzz} = \beta_{yyzz} = \beta_4$, $\beta_{xzxz} = \beta_{xzzx} = \beta_{yzyz} = \beta_{yzzy} = \beta_{zxxz} = \beta_{zxzx} = \beta_{zyyz} = \beta_{zyzy} = \beta_5$, $\beta_{zzxx} = \beta_{zzyy} = \beta_6$. So, the conductivity tensor σ of SWCT in the presence of the weak magnetic field $\boldsymbol{H}$, up to the square terms in the applied field, is of the form:

$$\sigma(\boldsymbol{H}) = \sigma + \begin{pmatrix} \beta_1 H_x^2 + \beta_3 H_y^2 + \beta_4 H_z^2 & \rho_1 H_z + (\beta_1 - \beta_3) H_x H_y & \rho_2 H_y + 2\beta_5 H_x H_z \\ -\rho_1 H_z + (\beta_1 - \beta_3) H_x H_y & \beta_3 H_x^2 + \beta_1 H_y^2 + \beta_4 H_z^2 & -\rho_2 H_x + 2\beta_5 H_y H_z \\ -\rho_2 H_y + 2\beta_5 H_x H_z & \rho_2 H_x + 2\beta_5 H_y H_z & \beta_6 (H_x^2 + H_y^2) + \beta_2 H_z^2 \end{pmatrix}.$$

TABLE II: **Symmetry of the tensors of SWCT.** The decompositions onto irreducible representations of the most frequent tensors (given in the last column) of the chiral (column 2) and the zig-zag and the armchair (column 3) SWCT. Tensors are obtained by multiplying polar and axial vectors, and the type of the products ($\otimes$, $[\dots]$ and $\{\dots\}$ for the direct, symmetrized and antisymmetrized) is in the first column. For $\mathcal{C}$ tubes $\kappa = 0$ for the km numbers and $\kappa = 2\pi r/qa$ for the $\tilde{k}\tilde{m}$ numbers.

Type	$\mathcal{C}$ tubes	$\mathcal{Z}$ and $\mathcal{A}$ tubes	Tensor
D^p	${}_0A^-_0 + {}_\kappa E_1$	${}_0A^-_0 + {}_0E^+_1$	r_i, p_i, E_i
$D^a = \{D^{a/p^2}\}$	${}_0A^-_0 + {}_\kappa E_1$	${}_0B^+_0 + {}_0E^-_1$	$l_i, H_i, R_{\{ij\}}$
D^{a/p^2}	$2{}_0A^+_0 + {}_0A^-_0 + 2{}_\kappa E_1 + {}_{2\kappa}E_2$	$2{}_0A^+_0 + {}_0B^+_0 + 2{}_0E^-_1 + {}_0E^+_2$	$\rho_{\{ij\}k}, R_{ij}$
$[D^{a/p^2}]$	$2{}_0A^+_0 + {}_\kappa E_1 + {}_{2\kappa}E_2$	$2{}_0A^+_0 + {}_0E^-_1 + {}_0E^+_2$	$\varepsilon_{[ij]}, \sigma_{[ij]}, R_{[ij]}$
$D^p \otimes D^a$	$2{}_0A^+_0 + {}_0A^-_0 + 2{}_\kappa E_1 + {}_{2\kappa}E_2$	${}_0A^-_0 + 2{}_0B^-_0 + 2{}_0E^+_1 + {}_0E^-_2$	$\gamma^A_{i\{jk\}}$
$D^p \otimes [D^{a/p^2}]$	${}_0A^+_0 + 3{}_0A^-_0 + 4{}_\kappa E_1 + 2{}_{2\kappa}E_2 + {}_{3\kappa}E_3$	$3{}_0A^-_0 + {}_0B^-_0 + 4{}_0E^+_1 + 2{}_0E^-_2 + {}_0E^+_3$	$\alpha_{[ij]k}, \gamma^S_{i[jl]}$
D^{p^3}	$3{}_0A^+_0 + 4{}_0A^-_0 + 6{}_\kappa E_1 + 3{}_{2\kappa}E_2 + {}_{3\kappa}E_3$	$4{}_0A^-_0 + 3{}_0B^-_0 + 6{}_0E^+_1 + 3{}_0E^-_2 + {}_0E^+_3$	γ_{ijk}
$[D^{a/p^2}] \otimes [D^{a/p^2}]$	$6{}_0A^+_0 + 2{}_0A^-_0 + 6{}_\kappa E_1 + 5{}_{2\kappa}E_2 + 2{}_{3\kappa}E_3 + {}_{4\kappa}E_4$	$6{}_0A^+_0 + 2{}_0B^+_0 + 6{}_0E^-_1 + 5{}_0E^+_2 + 2{}_0E^-_3 + {}_0E^+_4$	$\beta_{[ij][kl]}$

In general, the Raman (polarizability) tensor R_{ij} relates induced polarization to the external electric field[18]: $P_i = \sum_j R_{ij} E_j$. Therefore, the Table II combined with (A2) gives the selection rules of the Raman scattering: the relevant transitions are between the states with km-numbers $k_f - k_i = 0$ and $\Delta m = m_f - m_i = 0, \pm 1, \pm 2$; for the achiral tubes z-reversal parity of these states is different if $\Delta m = 1$ and same if Δm even. For the frequently important symmetric part $R_{[ij]}$ and its anisotropic component $R^{\mathrm{a}}_{[ij]}$ (the last one transforms according to $[D^{p^2}] - {}_0A^+_0$), the momenta selection rules are same, while both the z-reversal (and the vertical mirror for achiral tubes) parity is conserved if $\Delta m = 0$. The isotropic component $R^s_{[ij]}$ transforms according to the identity representation ${}_0A^+_0$, and involves only the transitions between the states with the coincident quantum numbers. As for the antisymmetric part, $R_{\{ij\}}$, $\Delta m = 0, \pm 1$; if $\Delta m = 0$ the relevant transitions are between the states with opposite U-parity for the chiral tubes and equal horizontal mirror parity but the opposite vertical mirror parity in the achiral cases. Of course, in the concrete calculations, these rules can be further specified according to the incident light polarization and direction.

V. CONCLUDING REMARKS

The assignation of the energy bands of SWCT by the complete set of the symmetry based quantum numbers is discussed. The quantum numbers k, m (or $\tilde{k}$, $\tilde{m}$) and parities $\pm$ and A/B are related to specific symmetries of SWCT. When parametrized by the quasi momentum k, the bands carry the quantum number of the angular momentum m, while in the parametrization by the helical momentum $\tilde{k}$ only the uncoupled to the translations part $\tilde{m}$ of the angular momentum characterizes the bands. The ranges of m and $\tilde{m}$ have been redefined compared to the one used in the nanotube literature[2,3] to get the standard quantum mechanical interpretation of the z-projection of the orbital angular momentum. The momenta quantum numbers are imposed by the roto-translational subgroup $\boldsymbol{L}^{(1)} = \boldsymbol{T}_r^q \boldsymbol{C}_n$, and characterize all the quasi 1D crystals. Indeed, in their symmetry $\boldsymbol{L}^{(1)}$ is always present as the maximal abelian part, thus causing no degeneracy. Additional U and $\sigma_{\rm v}$ parities of SWCT introduce band degeneracy. Relating the quantum numbers to the irreducible representations of the symmetry groups this assignation immediately gives the band degeneracies and information on non-accidental band sticking.

The bands have specific symmetry with respect to the $k = 0$ and $k = \pi/a$; therefore, the irreducible domain sufficient to characterize the entire band is the non-negative half of the Brillouin zone $[0, \pi]$. At the edge points $k = 0, \pi/a$, either the band stick to the another one or the corresponding eigen state gets z-reversal parity $\pm$. The U-axis symmetry reverses both the linear and angular momenta causing at least double degeneracy of the bands in the interior of the ID. For the $\mathcal{Z}$ and $\mathcal{A}$ tubes, the vertical mirror plane implies degeneracy of m and $-m$ bands. Thus the bands are four-fold degenerate, except $m = 0, n$ ones, which are $\sigma_{\rm v}$ odd or even and double degenerate.

At $k = 0$ m and $-m$ bands are sticked together. The symmetry of the screw axis imposes additional band sticking: the set of q/n bands is pairwise (m and $-p-m$ at $k = \pi/a$ and $\pm m$ at $k = 0$) sticked together. These bands are continued in a single band in the q/n times extended Brillouin zone corresponding to the $\tilde{k}\tilde{m}$ quantum numbers. Only the bands ending up with U-parity even or odd states are not sticked to the another ones, with the van Hove singularities and the halved degeneracy at the end points.

These conclusions are generally valid for any (quasi)particle energy bands of SWCT. All other bands sticking or increased degeneracy, if any, are accidental, i.e. related to the hamiltonian under study. Note that only within spin independent models the U-axis imposed double degeneracy coincides with that introduced by the time reversal symmetry, since both operations reverse linear and orbital angular momenta.

According to this general scheme the complete assignation of the SWCT electronic tight-binding bands is performed. The generalized Bloch functions are found and characterized by the full set of ($km\Pi$), or, alternatively, ($\tilde{k}\tilde{m}\Pi$), quantum numbers. All these functions contain two parts: the two halves of SWCT consisting of C_{ts0} and C_{ts1} atoms (black and white ones in the Fig. 1) contribute to the state by different phase factors. This form is useful in calculations and comparison to the STM images[19], again manifests the existence of the U-symmetry which interrelate the two halves.

A brief comment on the SWCT conductivity within the present context may enlighten some of the discussed questions. Recall that the simplest (tight-binding nearest neighbors and homogeneous distortions) model with the bands given in the Table I, predicts[2,3] that the tubes with $n_1 - n_2$ divisible by 3 should be conductors due to the crossing of the two bands[20] $\tilde{m}_F = 0$ if $\mathcal{R} = 3$ and $\tilde{m}_F = (-1)^{\mathrm{Fr}(r/3)} n/3$ for $\mathcal{R} = 1$ at $\tilde{k}_F = 2\pi/3$. Alternatively, in km numbers, when $\mathcal{R} = 3$ then $k_F = 2\pi/3$ and $m_F = nr \pmod q$, while $k_F = 0$ and $m_F = \pm q/3$ for $\mathcal{R} = 1$. This extra degeneracy at the Fermi level is a model dependent accidental one, being not induced by symmetry. On the contrary, the symmetry based non-crossing rule just prevents the conductivity except in the armchair tubes, since the momenta quantum numbers of the crossing bands are the same; only for the armchair tubes, when $m_F = n$ these bands also carry the opposite vertical mirror parity. So, as verified experimentally[21] and in the more subtle theoretical models[20], the secondary gap must be opened except for the armchair tubes, for which the accidental crossing point k_F is shifted to the left. In these cases the metallic plato[19,22] is ended by the systematic van Hove singularities.

The major benefit from the complete assignation of bands and corresponding generalized Bloch functions comes from the selection rules. The momenta conservation selection rules (A1) emerge from the roto-translational subgroup $\boldsymbol{T}_q^r \boldsymbol{C}_n$ making these rules also applicable to all other nanotubes (multi-wall, BN, etc.) and stereoregular polymers. The novel conserved parities refine the momenta conservation rules. The coincidence of the z-reversal odd and even states with the systematic van Hove singularities proves substantial influence of the parities to the physical processes in nanotubes and related spectra[23,16]. Therefore, these additional rules must not be overlooked in calculations.

To illustrate further the relevance of the derived parity selection rules, let us briefly discuss armchair tubes and the parallel component of the dielectric tensor $\epsilon_{ij}(\boldsymbol{k}, \omega)$, which is the corner stone in the analysis of various optical properties[16]. The contribution of the direct interband transitions caused by the electric field along the z-axis are to be included in calculations. As the perturbation field has odd z-reversal and even vertical mirror parities, it transforms according to the representation ${}_0A_0^-$. Therefore, the absorption may be realized only by the (vertical) transitions $\epsilon_m^-(k) \to \epsilon_m^+(k)$, and this exhausts

the selection rules imposed by the roto-translational subgroup. Nevertheless, the eigen states of the pairs of the double degenerate bands with $m = 0, n$ have different $\sigma_{\rm v}$ parity, and the transitions between these bands are forbidden for any k. Thus, only the transitions between the four fold degenerate ${}_kG_m$ bands are allowed for z polarized light. Also in the Raman scattering processes the selection rules besides the momenta strongly involve parities.

Finally, the tensor properties of some physical quantities were established, to make the use of the selection rules quite straightforward. We emphasize that the considered tensors interrelate vector (polar or axial) quantities making that all of them are associated to quantum number $k = 0$. This provides full conservation of momenta (e.g. vertical optical transitions), even when the km-numbers are used (where m is not conserved in general). On the other side, the selection rules with the conserved $\tilde{k}\tilde{m}$ numbers are more compact and easy to deal with. Nevertheless, some components of the relevant tensors have non-vanishing $\tilde{k}$, which makes some results less obvious. For example, some optical transitions are not vertical in $\tilde{k}$.

APPENDIX A: CLEBSCH-GORDAN COEFFICIENTS

The Clebsch-Gordan coefficients are given for the irreducible representations of the line groups $\boldsymbol{L}_{\mathcal{C}}$ and $\boldsymbol{L}_{\mathcal{A}}$ presented in Ref. 7. Besides the pair (k, m) of linear and z-component of the angular momenta (or $(\tilde{k}, \tilde{m})$ of helical and pure angular momenta), some of the irreducible representations carry also the quantum numbers of parities with respect to the U axis, and mirror planes $\sigma_{\rm v}$ or $\sigma_{\rm h}$. Thus the following Clebsch-Gordan coefficients reflect the conservation laws of these quantities.

The addition of quasi momenta is performed modulo their range, which is indicated by $\doteq$:

$$k + k_i \doteq k + k_i + 2K\pi/a, \tag{A1a}$$
$$m + m_i \doteq m + m_i + Mq, \tag{A1b}$$
$$\tilde{k} + \tilde{k}_i \doteq \tilde{k} + \tilde{k}_i + 2\tilde{K}\tilde{\pi}, \tag{A1c}$$
$$\tilde{m} + \tilde{m}_i \doteq \tilde{m} + \tilde{m}_i + \tilde{M}n, \tag{A1d}$$

where K, M, $\tilde{K}$ and $\tilde{M}$ are the integers providing the results in BZ, $(-q/2, q/2]$, $\widetilde{\rm BZ}$ and $(-n/2, n/2]$, respectively. In the following expressions the value of the parities Π may be ± 1 for even and odd states or 0 for all the other states with undefined parity. When this value is explicitly given (or absent) in expression, the other quantum numbers are restricted to the compatible values. For given values (k, m, Π) and (k_i, m_i, Π_i) (or $(\tilde{k}, \tilde{m}, \Pi)$ and $(\tilde{k}_i, \tilde{m}_i, \Pi_i)$) the Clebsch-Gordan coefficients are non-vanishing iff $k_f \doteq k + k_i$ and $m_f \doteq m + m_i + pK$, where $K = (k + k_i - k_f)a/2\pi$ is an integer, i.e. $\tilde{k}_f \doteq \tilde{k} + \tilde{k}_i$ and $\tilde{m}_f \doteq \tilde{m} + \tilde{m}_i$, and $\Pi_f = \Pi\Pi_i$ when both Π and Π_i are defined. For $\mathcal{Z}$ and $\mathcal{A}$ tubes $p = n$ and $\Pi_f = \Pi\Pi_i$ refers to conservation of each parities separately. In all these cases the value of the CG coefficient is 1,

$$\langle k_f, m_f, \Pi_f \mid km\Pi; k_i m_i \Pi_i \rangle = \langle \tilde{k}_f, \tilde{m} m_f, \Pi_f \mid \tilde{k}\tilde{m}\Pi; \tilde{k}_i \tilde{m}_i \Pi_i \rangle = 1, \tag{A2}$$

with the following exceptions:

1. Chiral tubes, $\tilde{k}\tilde{m}$-numbers:

$$\begin{array}{ll} \langle \tilde{k}_f, \tilde{m}_f \mid \tilde{k}\tilde{m}; \tilde{k}_i \tilde{m}_i - \rangle & -1, \text{ if } \tilde{k} < 0, \text{ or } \tilde{k} = 0, \tilde{\pi}, \tilde{m} < 0; \\ \langle \tilde{k}_f, \tilde{m}_f \mid \tilde{k}\tilde{m} -; \tilde{k}_i \tilde{m}_i \rangle & = -1, \text{ if } \tilde{k}_i < 0, \text{ or } \tilde{k}_i = 0, \tilde{\pi}, \tilde{m}_i < 0; \\ \langle \tilde{k}_f, \tilde{m}_f, \pm \mid \tilde{k}, \tilde{m}; \tilde{k}_i, \tilde{m}_i \rangle & = \begin{cases} \pm\frac{1}{\sqrt{2}}, & \tilde{k} < 0, \text{ or } \tilde{k} = 0, \tilde{\pi}, \tilde{m} < 0, \\ \frac{1}{\sqrt{2}}, & \text{otherwise.} \end{cases} \end{array} \tag{A3}$$

2. Chiral tubes, km-numbers:

$$\begin{array}{ll} \langle k_f, m_f \mid km; k_i m_i - \rangle & = -1, \text{ if } k < 0, \text{ or } k = 0, m < 0, \text{ or } k = \pi/a, m \notin [-\frac{p}{2}, \frac{q-p}{2}]; \\ \langle k_f, m_f \mid km -; k_i m_i \rangle & = -1, \text{ if } k_i < 0, \text{ or } k_i = 0, m_i < 0, \text{ or } k_i = \pi/a, m_i \notin [-\frac{p}{2}, \frac{q-p}{2}]; \\ \langle k_f, m_f, \pm \mid k, m; k_i, m_i \rangle & = \begin{cases} \pm\frac{1}{\sqrt{2}}, & k < 0, \text{ or } k = 0, m < 0 \text{ or } k = \pi, m_i \notin [-\frac{p}{2}, \frac{q-p}{2}], \\ \frac{1}{\sqrt{2}}, & \text{otherwise.} \end{cases} \end{array} \tag{A4}$$

3. Achiral tubes (only the cases with $k = 0$ are considered; θ_x is the negative step function, being 1 when $x < 0$

and zero otherwise; especially θ_{Π^s} is shorten to θ_s, for $s = h, v, U$):

$$
\begin{aligned}
&\langle 0, m_f, \Pi^h\Pi^{h_i} \mid 0, m, B, \Pi^h; 0, m_i, \Pi^{h_i} \rangle && = -1, \text{ if } m_i < 0;\\
&\langle 0, m_f, \Pi^h\Pi^{h_i} \mid 0, m, \Pi^h; 0, m_i, B, \Pi^{h_i} \rangle && = -1, \text{ if } m < 0;\\
&\langle 0, m_f, \Pi^v\Pi^{v_i} \mid 0, m, \Pi^v, -; k_i, m_i, \Pi^{v_i} \rangle = \langle k_i, m_f \mid 0, m, -; k_i, m_i \rangle && = -1, \text{ if } k_i < 0;\\
&\langle \pi/a, m_f, -\Pi^h\Pi^{U_i} \mid 0, m, B, \Pi^h; \pi/a, -n/2, \Pi^{U_i} \rangle && = -1;\\
&\langle k_f, m_f \mid 0, m, \Pi^v, \Pi^h; k_i, m_i \rangle = \langle k_f, m_f \mid 0, m, \Pi^h; k_i, m_i \rangle && = (-1)^{\theta_h\theta_{k_i}+\theta_v\theta_{m_i}};\\
&\langle \pi/a, m_f \mid 0, m, \Pi^h; \pi/a, m_i, \Pi^{U_i} \rangle && = (-1)^{(\theta_h+\theta_{U_i})(\theta_m+\theta_{m_i})};\\
&\langle 0, m_f, \Pi^v, \Pi^h\Pi^{h_i} \mid 0, m, \Pi^h; 0, m_i, \Pi^{h_i} \rangle && = \tfrac{(-1)^{\theta_v\theta_m}}{\sqrt{2}};\\
&\langle \tfrac{\pi}{a}, m_f, \Pi^{U_f} \mid 0, m, \Pi^h; k_i, 0, \Pi^{v_i} \rangle && = \tfrac{(-1)^{(\theta_{U_f}+\theta_h)\theta_{k_i}+\theta_{v_i}\theta_m}}{\sqrt{2}};\\
&\langle k_f, 0, \Pi^{v_f} \mid 0, m, \Pi^h; \tfrac{\pi}{a}, m_i, \Pi^{U_i} \rangle && = \tfrac{(-1)^{(\theta_{U_i}+\theta_h)(\theta_{m_i}+\theta_m)+\theta_{v_f}\theta_m}}{\sqrt{2}};\\
&\langle k_f, m_f, \Pi^{v_f} \mid 0, m, \Pi^h; k_i, m_i \rangle && = \tfrac{(-1)^{\theta_h\theta_{k_i}+\theta_{v_f}\theta_m}}{\sqrt{2}};\\
&\langle k_f, m_f, \Pi^{U_f} \mid 0, m, \Pi^h; k_i, m_i \rangle && = \tfrac{(-1)^{(\theta_{U_f}+\theta_h)\theta_{k_i}}}{\sqrt{2}}.
\end{aligned}
\tag{A5}
$$

REFERENCES

† Electronic address: tanja37@afrodita.rcub.bg.ac.yu; URL: `http://www.ff.bg.ac.yu/qmf/qsg_e.htm`

[1] S. Iijima, Nature, **354**, 56 (1991).

[2] Hamada, S. Sawada and A. Oshiyama, Phys. Rev. Lett. **68**, 1579 (1992); M. Dresselhaus, G. Dresselhaus and P. C. Eklund, *Science of Fullerenes and Carbon Nanotubes*, Academic Press, San Diego, 1998; R. Saito, G. Dresselhaus, M. Dresselhaus, *Physical Properties of Carbon Nanotubes* (Imp. College Press 1998).

[3] C. T. White, D. H. Robertson and J. W. Mintmire, Phys. Rev. B **47** 5485 (1993); C. T. White, T. N. Todorov, Nature **323**, 240 (1998); R. A. Jishi, L. Venkataraman, M. S. Dresselhaus and G. Dresselhaus, Phys. Rev. B, **16** 11176 (1995).

[4] M. Damnjanović, I. Milošević, T. Vuković and R. Sredanović, Phys. Rev. **B 60** (3) 2728-2739 (1999), J. Phys. A **32** 4097-4104 (1999).

[5] Note that for SWCT $\tilde{q} = q/n = 2 \pmod{12}$ is even; for $\mathcal{Z}$ and $\mathcal{A}$ tubes $\tilde{q} = 2$. Since n is also the greatest common divisor of q and p, n and p are simultaneously even only when both n_1 and n_2 are even.

[6] S. L. Altmann, *Band Theory of Solids. An introduction from the Point of View of Symmetry* (Clarendon Press, Oxford, 1991); S. S. L. Altmann, *Induced Representations in Crystals and Molecules* (London: Academic, 1977); J. P. Elliot and P. G. Dawber, *Symmetry in Physics* (London: Macmillan, 1979).

[7] M. Damnjanović, T. Vuković and I. Milošević, J. Phys. A **33** (2000) 6561-72.

[8] I. Milošević and M. Damnjanović, Phys. Rev., **B 47** 7805 (1993).

[9] The states and representations with $k = \pi/a$ and $\tilde{k} = \tilde{\pi}/a$ are for short labeled by π and $\tilde{\pi}$, respectively.

[10] The transition between the two sets of quantum numbers is obtained calculating the linear and the angular part of the momentum canonically conjugated to the helix generated by $(C_q^r|na/q)$. The pair $\tilde{k}\tilde{m}$ is equivalent to $k = \tilde{k} - 2\pi\tilde{m}r/na + 2K\pi/a$, $m = \tilde{m} - Kp + Mq$, while to the pair km correspond $\tilde{k} = k + 2\pi rm/na + 2\tilde{K}\tilde{\pi}/a$ and $\tilde{m} = m + \tilde{M}n$. The integers K, M, $\tilde{K}$ and $\tilde{M}$ provide the quasi momenta from the proposed intervals. They are independet except that M is a function of K, such that the change of k for 2π causes the change of m for $-p$ (for fixed $\tilde{k}\tilde{m}$). The transition rules enable also to derive the $\tilde{k}\tilde{m}$ numbers for the achiral tubes, which are in the literature treated only with km-numbers.

[11] S. Reich and C. Thomsen *Phys. Rev. B* **62**, 4273 (2000).

[12] J. C. Slater and G. F. Koster, *Phys. Rev.* **94** 1498 (1954); R. R. Sharma, *Phys. Rev.* **B19**, 2813-23 (1979); H. Eschrig, *Phys. Stat. Solidi (b)* **96**, 329 (1979); D. Porezag, Th. Frauenheim, Th. Köhler, G. Seifert and R. Kaschner, *Phys. Rev. B* **51** 12947 (1995).

[13] A. Messiah, *Quantum Mechanics* (Amsterdam: North-Holland, 1972).

[14] W. A. Wooster, *Tensors and Group Theory for the Physical Properties of Crystals* (Oxford: Clarendon, 1973); J. F. Nye, *Physical properties of crystals* (Oxford: Clarendon, 1964).

[15] L. D. Landau and E. M. Lifshic, *Electrodynamics of Continuous Media*, (London: Pergamon, 1963).

[16] S. Tasaki, K. Maekawa and T. Yamabe, Phys. Rev. B **57** 9301 (1998).

[17] M. Damnjanović, Phys. Lett. A **94** 337 (1983); I. Milošević, Phys. Lett. A **204** 63 (1995).

[18] M. Cardona, in *Light Scattering in Solids II*, edited by M. Cardona and G. Güntherodt (Springer, Berlin, 1982).

[19] A. Rubio, Appl. Phys. A **68** 275-82 (1999); A. Rubio, D. Sanchez-Portal, E. Artacho, P. Ordejon and J. M. Soler, Phys. Rev. Lett. **82** 3520-3 (1999).

[20] C. Kane and E. J. Mele, Phys. Rev. Lett. **78** 1932-5 (1997). M. Damnjanović, T. Vuković and I. Milosević, Solid State Comm. **116** 265-7 (2000).

[21] C. Zhou, J. Kong and H. Dai, Phys. Rev. Lett. **84** 5604-7 (2000).

[22] Ph. Lambin, V. Meunier and A. Rubio Phys. Rev. B **62** 5129- 5135 (2000);
[23] J. C. Charlier and Ph. Lambin, Phys. Rev. B **57** R15037 (1998).